Establishment and verification of the prediction model of soil wetting pattern size in vertical moistube irrigation

Yanwei Fan, Zhiwei Yang and Hujun Wei

ABSTRACT

To solve the difficulty of observing the soil wetting pattern of vertical moistube irrigation, the HYDRUS-2D software is used to simulate wetting pattern data under different conditions. Based on the analysis of Origin 9.0 and summarizing the law of simulation data, an empirical model for predicting wetting pattern size is constructed, with the reliability of the model verified by experimental data. The results show that the power function is used to fit the relationship between the size of wetting pattern and irrigation time. The power function exponent has small changes in three directions (vertical upward, horizontal, and vertical downward) of the moistube. Further analysis shows that the power function coefficient is in accordance with the power function relationship with soil-saturated hydraulic conductivity, the steady permeability of the moistube, and the difference between soil-saturated moisture content and initial moisture content. The average absolute error of statistical indicators of the built model is between 0.30 and 1.42 cm, the root mean square error is between 0.42 and 1.65 cm, and the Nash–Sutcliffe efficiency coefficient is not less than 0.93. The model has a good prediction effect and can provide a scientific basis for the design, operation, and management of the moistube irrigation engineering.

Key words | HYDRUS-2D, predictive model, soil, vertical moistube irrigation, wetting pattern size

Yanwei Fan (corresponding author)
Zhiwei Yang
Hujun Wei
College of Energy and Power Engineering,
Lanzhou University of Technology,
Lanzhou 730050,
China
E-mail: *fanyanwei24@163.com*

HIGHLIGHTS

- Based on Origin 9.0 analysis and summarizing the law of the simulation data, a simplified empirical model for predicting the size of the soil wetting pattern is constructed, and was verified by experimental data.
- The model can well predict the size of soil wetting pattern under vertical moistube irrigation, and provide scientific basis for the optimization of the moistube irrigation engineering.

INTRODUCTION

Vertical moistube irrigation is a new type of moistube irrigation technology that uses a polymer semi-permeable membrane to make a moistube, through which water seeps out for continuous underground irrigation (Quinones-Bolanos *et al.* 2005; Yang 2010). Vertical moistube irrigation has the advantages over underground drip irrigation of deeper wetting depth, free setting spacing, low working head, and low power consumption. It is more suitable for deep-rooted plants and can keep the soil around the root system moist.

The volume of moist soil is an important basis for optimizing the spacing of irrigation devices, horizontal arrangement, and choosing a suitable irrigation system, and it is also one of the most important factors in the design of irrigation systems. Studies have shown that the wetting depth in the soil profile of the surface drip irrigation

doi: 10.2166/ws.2020.326

and the wetting radius of the soil surface are the main components of the soil wetting pattern (Dabral *et al.* 2012; Al-Ogaidi *et al.* 2016a), and that the main components of the soil wetting pattern of subsurface drip irrigation are the wetting depth, wetting radius, and upward wetting distance in the soil profile (Yao *et al.* 2011). Vertical moistube irrigation is a buried irrigation technology, and the main components of the soil wetting pattern are similar to those of underground drip irrigation (Fan *et al.* 2018a). During irrigation, the size of the components of the wetting pattern must be determined according to the cross section of the wetting pattern and the volume of the wet soil (Fernandez-Galvez & Simmonds 2006). Domestic and foreign scholars have developed some analytical models (Philip 1984; Chu 1994; Cook *et al.* 2003; Moncef & Khemaies. 2016), HYDRUS-2D models (Brandt *et al.* 1971; Šimůnek *et al.* 2008), and empirical models (Malek & Peters 2011; Al-Ogaidi *et al.* 2016; Fan *et al.* 2018b) to quantify the wet soil volume. Researchers compared and evaluated the above three types of models (Kandelous & Šimůnek 2010; Subbaiah 2013). The results show that analytical and HYDRUS-2D models are usually employed to solve control flow equations under specific initial and boundary conditions. Analytical models are based on point source assumptions and special forms of homogeneous soil physical properties. The HYDRUS-2D model can realize a wide range of boundary conditions, including irregular boundaries and soil heterogeneity, improving the popularity of its analysis in the design of moistube irrigation systems. Kandelous & Šimůnek (2010) believe that HYDRUS-2D can estimate soil moisture distribution under drip irrigation conditions more accurately than analysis and empirical models. The model has been successfully applied to simulate the distribution of soil moisture under different irrigation methods. Although each empirical model is relatively simple in form, it is obtained by analyzing laboratory and field data using regression and dimensional analysis methods. The empirical formula is only applicable to specific irrigation techniques, such as the developed point source or line source drip irrigation wetted pattern size, and is not applicable to vertical moistube irrigation (Malek & Peters 2011). Therefore, the development of an empirical model that can predict the size of the soil wetting pattern of vertical moistube irrigation would provide a convenient and practical method for quantifying the size of the wetting pattern and solving the problem that the wetting pattern is difficult to observe.

The combination of numerical simulation and experimental verification is a common method for studying the laws of soil water movement. Numerical simulation can simulate the process of soil water movement under different soil characteristics and different technical elements (Saito *et al.* 2006; Han *et al.* 2015; Šimůnek *et al.* 2016). Experiments can verify the laws summarized by numerical simulation and improve the reliability of research results. Kanda *et al.* (2020) used the HYDRUS-2D model to numerically simulate the soil moisture distribution of two soil textures (ST; loamy sand and sandy clay loam) under horizontal moistube irrigation, and verified them with experiments, with the results showing that the simulated values are very consistent with the experimental observations. Fan *et al.* (2018c) verified the reliability of the HYDRUS-2D simulation results of horizontal moistube irrigation by using indoor soil box experimental data. On this basis, the dynamic changes of soil wetting pattern under different ST and loams with different initial water content (θ_0), pressure head (H), and depth of burial (D) were studied. The results show that the movement distance of the soil wet front conforms to the rule of vertical downward > horizontal direction > vertical upward, the contours of soil moisture content are all approximately concentric circles, and that the texture of the soil has a significant effect on the characteristics of the wet body. Zhang *et al.* (2016) explored the infiltration of water in different soil textures under the condition of horizontal moistube irrigation based on laboratory experiments, with the results showing that the cumulative infiltration amount was negatively correlated with the soil clay content, that the wetting front was an approximate circle centered on the moistube, and that the relationship between the distance and time of the wetting front was approximately a power function. Fan *et al.* (2018a) determined the specific flow calculation formula of the vertical moistube through indoor experiments, and verified the accuracy of HYDRUS-2D simulation. On this basis, using HYDRUS-2D simulation to study the influence of ST, θ_0, H, moistube length (L) and D on the characteristics of vertical moistube irrigation wetting pattern shows that the contour of the wetting pattern and the water content was approximately an ellipsoid around the moistube. ST has a significant impact on the wetting pattern, and with the increase of soil clay content, the volume of wet soil decreases. The θ_0, H, and L have a greater impact on the distance of the wetting front and the volume of the wet soil, and D affects the position of the wetting pattern.

In previous research (Fan *et al.* 2018a), the authors of this article conducted a qualitative study on the soil characteristic parameters and irrigation technical elements affecting the soil wetting pattern of vertical moistube irrigation. Based on the previous qualitative research on the influencing factors of the vertical moistube irrigation, this study increases the simulation volume and uses the HYDRUS-2D software to obtain the wetting pattern size data with different factors; the laws of the simulation data are analyzed and summarized to construct a simplified empirical model for predicting the size of the soil wetting pattern; and experimental data is used to verify the reliability of the model in order to provide a scientific basis for the design, operation, and management of the moistube irrigation engineering.

MATERIALS AND METHODS

Laboratory experiments

The silt loam in Qilihe District, Lanzhou, and the sandy loam and sandy clay loam in Minqin County, Wuwei, Gansu Province, are used for vertical moistube irrigation experiments, with the sampling locations shown in Figure 1. The saturated water content θ_s and saturated hydraulic conductivity K_s of the experimental soil are measured by the ring knife method and the constant head method, respectively. The experimental soil characteristic parameters and irrigation technical parameters are shown in Table 1.

The experiment device consists of five parts: a height adjustable stand, a mariotte bottle, a hydraulic hose, a moistube, and a soil box (Figure 2). The soil box is made of 10 mm thick plexiglass, and the size is 60 cm (length) × 60 cm (width) × 100 cm (height). There are multiple ventilation holes (diameter 2 mm) at the bottom of the soil box to prevent air resistance in the soil. In the test, the mariotte

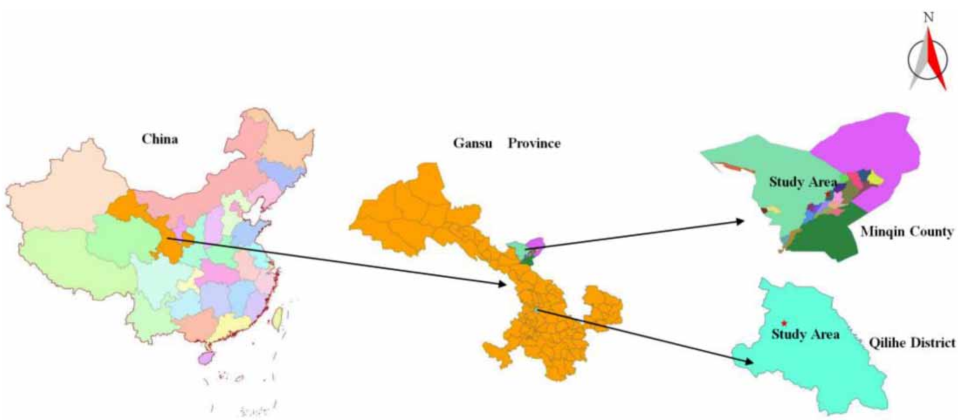

Figure 1 | Study area and the soil sampling locations in the study area situated in Gansu, China.

Table 1 | Characteristic parameters and irrigation technical parameters of experimental soils

ST	γ (g·cm^{-3})	K_s (cm·min^{-1})	θ_0 (cm^3·cm^{-3})	θ_s (cm^3·cm^{-3})	L (cm)	D (cm)	H (cm)
Silt loam	1.33	0.0143	0.147	0.450	20	30	150
					10	40	200
Sandy loam	1.56	0.0390	0.096	0.410	20	30	150
					10	40	200
Sandy clay loam	1.45	0.0305	0.158	0.390	20	30	150
					10	40	200

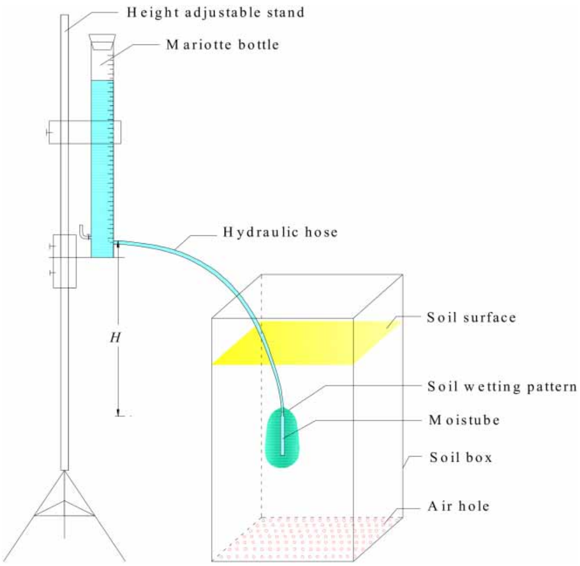

Figure 2 | Schematic diagram of experimental equipment (*H* represents inlet pressure head).

bottle provides a constant head, and the contour of the wetted body at different times is drawn with a marker.

Mathematical modeling

Basic equations

Vertical moistube irrigation is a spatial three-dimensional infiltration process under the condition of insufficient water supply, and the basic equation to soil water movement is the Richards equation (Richards 1931):

$$\frac{\partial \theta}{\partial t} = \frac{1}{r}\frac{\partial}{\partial r}\left[rK(h)\frac{\partial h}{\partial r}\right] + \frac{\partial}{\partial z}\left[K(h)\frac{\partial h}{\partial z}\right] - \frac{\partial K(h)}{\partial z} \quad (1)$$

where r is the radial coordinate (cm); z is the vertical coordinate (cm), which specifies that z is positive downward; θ is the soil moisture content (cm^3/cm^3); h is the pressure head (cm); t is the infiltration time (min); and $K(h)$ is the soil unsaturated hydraulic conductivity (cm/min).

The relationship among θ, h, and $K(h)$ in Equation (1) is fitted by the van Genuchten–Mualem (VG–M) model (van Genuchten 1980), which is:

$$\theta = \theta_\mathrm{r} + \frac{\theta_\mathrm{s} - \theta_\mathrm{r}}{(1 + |\alpha h|^n)^m} \quad (2)$$

$$K(h) = K_s S_e^l [1 - (1 - S_e^{1/m})^m]^2 \quad (3)$$

where S_e is the relative saturation of the soil, and $S_e = (\theta - \theta_r)/(\theta_s - \theta_r)$; θ_r is the residual soil moisture content (cm^3/cm^3); α is an empirical parameter, which is inversely proportional to the intake air value (cm^{-1}); n and m are empirical constants affecting the shape of the soil moisture characteristic curve, with $n > 1$ and $m = 1 - 1/n$; l is the empirical coefficient, usually 0.5.

The field water holding capacity is obtained using the prediction model established by Rab *et al.* (2011), and the specific expression is:

$$FC = 0.0805 + 1.68PWP - 1.62PWP^2 \quad (4)$$

where FC is the field water holding capacity (cm^3/cm^3), and PWP is the withering coefficient (cm^3/cm^3).

Naglič *et al.* (2014) showed that the withering coefficient of different soil textures can be expressed by the residual moisture content in the parameters of the VG–M model, namely:

$$PWP = \theta_r \quad (5)$$

Using Equations (4) and (5), we obtain:

$$FC = 0.0805 + 1.68\theta_r - 1.62\theta_r^2 \quad (6)$$

Initial and boundary conditions

Figure 3 shows the initial and boundary conditions considered when simulating different modeling scenarios in this study. Considering the axial symmetry of the vertical moistube, the area shown in Figure 3 is selected as the simulation calculation domain. The level of soil moisture content determines the rate of water movement in the soil. Therefore, in all simulation scenarios, the soil moisture content is set at a given initial moisture content.

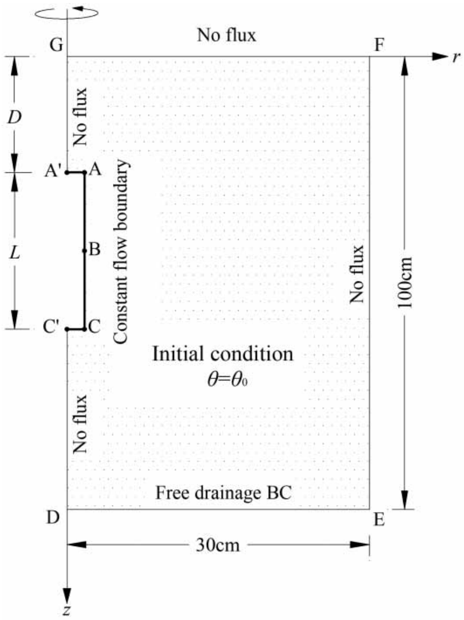

Figure 3 | The transport domain with applied initial and boundary conditions (D is the burial depth of moistube, L is the length of moistube, BC is the boundary condition).

The accurate setting of boundary conditions is critical to the simulation results. During the irrigation process, the surface soil is a dry soil layer, the amount of evaporation is very small, and therefore the influence of rainfall and evaporation is not considered at the upper boundary. When the simulation calculation domain is selected, the lower boundary is not affected by irrigation, and the left and right vertical boundaries are non-flux boundaries. During the irrigation process, the specific discharge of moistube (Q) at each node is basically constant (Niu *et al.* 2017; Fan *et al.* 2018a), and the Equation (7) established by Fan *et al.* (2018a) is used for the calculation:

$$q = K(H + M + a\gamma B + b) \quad (7)$$

where M is the distance between the computing node and the water inlet (cm); γ is the soil bulk density (g/cm^3); B is the buried depth of the calculation node (cm); a and b are the fitting parameters.

In summary, the initial conditions can be expressed as:

$$\theta(r, z, t) = \theta_0(r, z), 0 \le r \le 30 \text{ cm}, 0 \le z \le 100 \text{ cm}, t = 0 \quad (8)$$

where $\theta_0(r,z)$ is the initial soil moisture content (cm^3/cm^3).

The boundary conditions can be expressed as:

$$\begin{cases} -K(h)\dfrac{\partial h}{\partial z} + K(h) = 0, \ 0 \le r \le 30\,\text{cm}, \ z = 0 \,\text{or}\, z = 100\,\text{cm}, \ t \ge 0 \\ -K(h)\dfrac{\partial h}{\partial r} = 0, \ r = 0, \ 0 \le z \le D \,\text{or}\, (D + \text{L}) \le z \le 100\,\text{cm}, \ t \ge 0 \\ -K(h)\dfrac{\partial h}{\partial r} = 0, \ r = 30\,\text{cm}, \quad 0 \le z \le 100\,\text{cm}, \ t \ge 0 \\ -K(h)\dfrac{\partial h}{\partial r} = \dfrac{Q}{\pi d}, \ r = 0, \ D \le z \le (D + L), \ t \ge 0 \end{cases} \quad (9)$$

where d is the diameter of moistube (cm).

Simulation scheme

In order to construct an empirical model of the size of the soil wetting pattern of vertical moistube irrigation, seven STs are selected. For each ST, the settings are as follows: three initial water content (60%*FC*, 70%*FC*, and 80%*FC*), three lengths of moistube (10, 15, and 20 cm), three buried depths of moistube (20, 30, and 40 cm) and three pressure heads (100, 150, and 200 cm), a total of 63 groups. During the simulation, the irrigation time is set to 192 h. The field water holding capacity of the soil is calculated using Equation (6), and Q is obtained using Equation (7). The parameters of VG–M model of ST were taken from Carsel and Parrish's data (Carsel & Parrish 1988), and the soil bulk density γ was taken from Pachepsky and Park's data (Pachepsky & Park 2015).

Analysis method

Studies have shown that the maximum size of soil wetting patterns in different directions must be considered when describing soil wetting patterns (Kilic 2018). The maximum sizes of the soil wetting pattern in the vertical upward, horizontal, and vertical downward directions are located at the highest point (point A), the middle point (point B), and the lowest point (point C) of the moistube, respectively (as shown in Figure 3). Therefore, the three characteristic values – vertical upward, horizontal direction, and vertical downward – are selected to describe the soil wetting pattern of vertical moistube irrigation. Many scholars have found that the migration process of point source and line source infiltration can be described by power function with high accuracy

(Nagličet al. 2014; Al-Ogaidi et al. 2016a). Therefore, in this study, a power function is used to quantitatively analyze the migration process of the soil wetting pattern of vertical moistube irrigation, and the specific expression is:

$$Z_A = a_1 t^{b_1} \tag{10}$$

$$R_B = a_2 t^{b_2} \tag{11}$$

$$Z_C = a_3 t^{b_3} \tag{12}$$

where Z_A is wetting pattern dimensions of vertical upward (cm); R_B is wetting pattern dimensions of horizontal (cm); Z_C is wetting pattern dimensions of vertical downward (cm); and a_1, a_2, a_3, b_1, b_2, and b_3 are all fitting parameters.

Error analysis

The coefficient of determination R^2 is used to judge the fitness of Equations (10)–(12). R^2 is between 0 and 1; the closer R^2 is to 1, the better the fitting effect of the fitting equation. The mean absolute error (MAE), root mean square error (RMSE), and Nash–Sutcliffe efficiency coefficient (NSE) are used to evaluate the performance of the empirical model. If the comparison result shows that MAE and RMSE are closer to 0, and NSE is closer to 1, it indicates that the empirical model has good predictive performance. The parameters R^2, RMSE, MAE, and NSE are calculated using the following equations (Moriasi et al. 2007):

$$R^2 = \frac{\left(N\sum_{i=1}^{N} O_i C_i - \sum_{i=1}^{N} C_i \sum_{i=1}^{N} O_i\right)^2}{\left(N\sum_{i=1}^{N} (C_i)^2 - \left(\sum_{i=1}^{N} C_i\right)^2\right)\left(N\sum_{i=1}^{N} (O_i)^2 - \left(\sum_{i=1}^{N} O_i\right)^2\right)} \tag{13}$$

$$\text{MAE} = \frac{1}{N}\sum_{i=1}^{N} |O_i - C_i| \tag{14}$$

$$\text{RMSE} = \sqrt{\frac{1}{N}\sum_{i=1}^{N} (O_i - C_i)^2} \tag{15}$$

$$\text{NSE} = 1 - \frac{\sum_{i=1}^{N} (O_i - C_i)^2}{\sum_{i=1}^{N} (O_i - O_m)^2} \tag{16}$$

where O_i is the ith measured value; C_i is the ith calculated value; O_m is the average value of the measured value; and N is the total number of data.

RESULTS AND DISCUSSION

Parameter determination

Wetting pattern size of vertical upward

Based on the HYDRUS-2D simulation results, using Equation (10), the fitting parameters a_1 and b_1 in different influencing factor combinations are obtained through Origin 9.0 fitting. The fitting results are shown in Table 2. It can be seen from Table 2 that using Equation (10) to fit the relationship between the vertical upward wetting pattern size of vertical moistube irrigation and the irrigation time, $R^2 \geq 0.985$. It shows that Equation (10) demonstrates the relationship between the vertical upward wetting pattern size of vertical moistube irrigation and irrigation time.

Fitting parameter b_1

Table 2 shows that ST, θ_0, H, L, and D have little influence on the values of fitting parameter b_1, which fluctuate around the average value 0.476, and the fluctuation range is small. To simplify the calculation, the average value of the fitting parameter b_1 can be taken. Therefore, Equation (10) can be further expressed as:

$$Z_A = a_1 t^{0.476} \tag{17}$$

Fitting parameter a_1

A further analysis of Table 2 finds that the value of the fitting parameter a_1 varies in a small range. However, previous studies have found that the size of the soil wetting pattern of vertical moistube irrigation is mainly affected by ST, θ_0, H, L, and D, while H, L, and D affect Q, which in turn affects the size of the wetting pattern (Fan et al. 2018a). Therefore, taking the parameter a_1 as the average value alone does not meet the actual situation, nor can it meet the requirements for model universality. It is worth

Table 2 | Parameter values of a_1 and b_1, and coefficients of determination (R^2)

				Silt loam			Silt			Clay loam		
H (cm)	**L (cm)**	**D (cm)**	**θ_0 (cm³/cm³)**	a_1	b_1	R^2	a_1	b_1	R^2	a_1	b_1	R^2
150	15	20	80%*FC*	0.124	0.542	0.993	0.131	0.538	0.993	0.145	0.486	0.991
150	20	30	60%*FC*	0.151	0.509	0.992	0.145	0.512	0.992	0.160	0.506	0.992
150	20	30	70%*FC*	0.183	0.489	0.991	0.150	0.511	0.992	0.176	0.495	0.992
150	20	30	80%*FC*	0.196	0.473	0.991	0.187	0.481	0.991	0.209	0.470	0.991
150	15	30	80%*FC*	0.210	0.462	0.991	0.200	0.470	0.991	0.226	0.459	0.990
200	20	30	80%*FC*	0.241	0.465	0.991	0.240	0.469	0.991	0.242	0.471	0.991
100	20	30	80%*FC*	0.160	0.468	0.991	0.145	0.486	0.991	0.154	0.480	0.991
150	10	30	80%*FC*	0.250	0.434	0.989	0.231	0.447	0.990	0.252	0.439	0.990
150	10	40	80%*FC*	0.219	0.443	0.990	0.212	0.450	0.990	0.233	0.441	0.990
				Loamy sand			**Loam**			**Sandy clay loam**		
H (cm)	**L (cm)**	**D (cm)**	**θ_0 (cm³/cm³)**	a_1	b_1	R^2	a_1	b_1	R^2	a_1	b_1	R^2
150	15	20	80%*FC*	0.257	0.424	0.989	0.134	0.532	0.993	0.154	0.507	0.992
150	20	30	60%*FC*	0.218	0.438	0.990	0.141	0.511	0.992	0.146	0.501	0.992
150	20	30	70%*FC*	0.221	0.436	0.989	0.149	0.508	0.992	0.144	0.505	0.992
150	20	30	80%*FC*	0.229	0.433	0.989	0.175	0.491	0.992	0.168	0.489	0.991
150	15	30	80%*FC*	0.230	0.432	0.989	0.180	0.486	0.991	0.173	0.485	0.991
200	20	30	80%*FC*	0.290	0.415	0.989	0.208	0.484	0.991	0.203	0.480	0.991
100	20	30	80%*FC*	0.168	0.452	0.990	0.141	0.496	0.992	0.130	0.499	0.992
150	10	30	80%*FC*	0.234	0.430	0.989	0.198	0.471	0.991	0.188	0.472	0.991
150	10	40	80%*FC*	0.212	0.436	0.989	0.188	0.471	0.991	0.167	0.479	0.991
				Sandy loam								
H (cm)	**L (cm)**	**D (cm)**	**θ_0 (cm³/cm³)**	a_1	b_1	R^2						
150	15	20	80%*FC*	0.163	0.494	0.992						
150	20	30	60%*FC*	0.162	0.486	0.991						
150	20	30	70%*FC*	0.161	0.487	0.991						
150	20	30	80%*FC*	0.167	0.485	0.991						
150	15	30	80%*FC*	0.172	0.481	0.991						
200	20	30	80%*FC*	0.209	0.470	0.991						
100	20	30	80%*FC*	0.131	0.495	0.992						
150	10	30	80%*FC*	0.183	0.472	0.991						
150	10	40	80%*FC*	0.164	0.478	0.991						

considering that Q at different buried depths is different, and due to the influence of gravity, the discharge flow of the adjacent points above and below the moistube will have a superposition effect. Therefore, Q alone cannot fully reflect the water permeability of the moistube, and the product of the average specific flow rate (q) of the moistube and L can be used to characterize the water permeability of the moistube. The θ_0 has a certain influence on the size of the wetting pattern; the influence mechanism is that during the irrigation process, the irrigation water moves around in the soil pores, and gradually fills the soil pores until the soil is fully saturated. Therefore, the final determination of the size of the wetting pattern is the amount of water required to fill the pores of the soil to achieve approximate saturation. It can be expressed by the difference between θ_s and θ_0, that is, θ_s–θ_0. In addition, the influence of ST on the size of the wetting pattern can be characterized by K_s. Therefore, the influencing factors of the simplified vertical moistube irrigation soil wetting pattern size mainly include K_s, qL, and (θ_s–θ_0).

Based on this, the function expression of fitting parameter a_1 is established by multiple regression analysis as follows:

$$a_1 = \lambda_1(\theta_s - \theta_0)^{c_1} K_s^{d_1} (qL)^{e_1} \tag{18}$$

where λ_1, c_1, d_1, and e_1 are all empirical parameters.

Wetting pattern size of horizontal

Table 3 shows the simulation results based on HYDRUS-2D. Using Equation (11), the values of fitting parameters a_2 and b_2 under different influencing factor combinations and R^2 are obtained by fitting with Origin 9.0. It can be seen from Table 3 that using Equation (11) to fit the relationship between the horizontal wetting pattern size of vertical moistube irrigation and the irrigation time gives $R^2 \geqq 0.985$, indicating that Equation (11) demonstrates the relationship between the horizontal wetting pattern size of vertical moistube irrigation and the irrigation time.

Fitting parameter b_2

A comparative analysis of Table 3 finds that ST, θ_0, H, L, and D also have little effect on the value of the fitting parameter b_2, all fluctuating around 0.406 on the average. To simplify the calculation, the average value of the fitting parameter b_2 is taken. Therefore, Equation (11) can be further expressed as:

$$R_B = a_2 t^{0.406} \tag{19}$$

Fitting parameter a_2

A further analysis of Table 3 finds that the fitting parameter a_2 is affected by ST, θ_0, H, L, and D, and that the value fluctuates greatly. The size of the horizontal wetting pattern is a component of the size of the soil wetting pattern of the vertical moistube irrigation, and the analysis of the fitting parameter a_1 shows that the factors affecting the size of the soil wetting pattern of the vertical moistube irrigation have been simplified to K_s, qL, and (θ_s–θ_0). Therefore, the functional expression of the fitting parameter a_2 can be established by multiple regression analysis, which is:

$$a_2 = \lambda_2(\theta_s - \theta_0)^{c_2} K_s^{d_2} (qL)^{e_2} \tag{20}$$

where λ_2, c_2, d_2, and e_2 are all empirical parameters.

Wetting pattern size of vertical downward

Using the HYDRUS-2D simulation results and Equation (12), the fitting parameters a_3 and b_3 under different combinations of influencing factors were obtained by Origin 9.0. The values of parameters a_3 and b_3 and R^2 are shown in Table 4. It can be seen from Table 4 that Equation (12) is used to fit the relationship between wetting pattern dimension of vertical downward of vertical moistube irrigation and irrigation time, and $R^2 \geqq 0.989$, indicating that Equation (12) demonstrates the relationship between wetting pattern dimension of vertical downward of vertical moistube irrigation and irrigation time.

Fitting parameter b_3

A comparative analysis of Table 4 shows that ST, θ_0, H, L, and D also have a small effect on the value of the fitting parameter b_3, all fluctuating around 0.428 on average. In order to simplify the calculation, the average value of the fitting parameter is taken as b_3. Equation (12) can be expressed as:

$$Z_C = a_3 t^{0.428} \tag{21}$$

Fitting parameter a_3

A further analysis of Table 4 finds that the value of the fitting parameter a_3 fluctuates greatly, with ST, θ_0, H, L, and D all affecting it. The vertical downward wetting pattern size and the vertical upward and horizontal wetting pattern size can completely describe the vertical moistube irrigation soil wetting pattern. According to the analysis of fitting parameters a_1

Table 3 | Parameter values of a_2 and b_2, and coefficients of determination (R^2)

				Silt loam			Silt			Clay loam		
H (cm)	L (cm)	D (cm)	θ_0 (cm³/cm³)	a_2	b_2	R^2	a_2	b_2	R^2	a_2	b_2	R^2
150	15	20	80%FC	0.697	0.383	0.987	0.661	0.390	0.987	0.492	0.410	0.988
150	20	30	60%FC	0.442	0.436	0.989	0.431	0.436	0.989	0.495	0.427	0.989
150	20	30	70%FC	0.495	0.426	0.989	0.463	0.431	0.989	0.529	0.421	0.989
150	20	30	80%FC	0.613	0.402	0.988	0.572	0.411	0.988	0.655	0.398	0.988
150	15	30	80%FC	0.728	0.373	0.986	0.642	0.389	0.987	0.693	0.383	0.987
200	20	30	80%FC	0.664	0.406	0.988	0.632	0.411	0.988	0.699	0.404	0.988
100	20	30	80%FC	0.513	0.404	0.988	0.492	0.410	0.988	0.548	0.400	0.988
150	10	30	80%FC	0.747	0.357	0.985	0.713	0.364	0.986	0.802	0.351	0.985
150	10	40	80%FC	0.719	0.354	0.985	0.676	0.364	0.986	0.717	0.358	0.986

				Loamy sand			Loam			Sandy clay loam		
H (cm)	L (cm)	D (cm)	θ_0 (cm³/cm³)	a_2	b_2	R^2	a_2	b_2	R^2	a_2	b_2	R^2
150	15	20	80%FC	0.679	0.384	0.987	0.577	0.407	0.988	0.477	0.425	0.989
150	20	30	60%FC	0.567	0.405	0.988	0.439	0.433	0.989	0.439	0.429	0.989
150	20	30	70%FC	0.570	0.404	0.988	0.451	0.433	0.989	0.447	0.430	0.989
150	20	30	80%FC	0.570	0.405	0.988	0.497	0.426	0.989	0.466	0.429	0.989
150	15	30	80%FC	0.612	0.391	0.987	0.537	0.409	0.988	0.516	0.411	0.988
200	20	30	80%FC	0.687	0.393	0.987	0.564	0.423	0.989	0.546	0.422	0.989
100	20	30	80%FC	0.438	0.421	0.989	0.419	0.430	0.989	0.378	0.436	0.989
150	10	30	80%FC	0.653	0.376	0.987	0.599	0.387	0.987	0.559	0.393	0.987
150	10	40	80%FC	0.592	0.382	0.987	0.576	0.388	0.987	0.379	0.43	0.989

				Sandy loam		
H (cm)	L (cm)	D (cm)	θ_0 (cm³/cm³)	a_2	b_2	R^2
150	15	20	80%FC	0.547	0.409	0.988
150	20	30	60%FC	0.462	0.425	0.989
150	20	30	70%FC	0.454	0.428	0.989
150	20	30	80%FC	0.471	0.427	0.989
150	15	30	80%FC	0.513	0.411	0.988
200	20	30	80%FC	0.547	0.420	0.989
100	20	30	80%FC	0.372	0.438	0.990
150	10	30	80%FC	0.550	0.395	0.988
150	10	40	80%FC	0.513	0.397	0.988

and a_2, the function expression of fitting parameter a_3 is established based on multiple regression analysis, which is:

$$a_3 = \lambda_3(\theta_s - \theta_0)^{c_3} K_s^{d_3} (qL)^{e_3} \quad (22)$$

where λ_3, c_3, d_3, and e_3 are all empirical parameters.

Establishment of the empirical model

Equations (18), (20), and (22) were substituted into Equations (17), (19), and (21), respectively. With 63 simulation data, the empirical model of soil wetting pattern dimensions under vertical moistube irrigation was obtained

Table 4 | Parameter values of a_3 and b_3, and coefficients of determination (R^2)

				Silt loam			Silt			Clay loam		
H **(cm)**	***L*** **(cm)**	***D*** **(cm)**	θ_0 **(cm³/cm³)**	a_3	b_3	R^2	a_3	b_3	R^2	a_3	b_3	R^2
150	15	20	80%*FC*	0.493	0.403	0.988	0.485	0.406	0.988	0.415	0.396	0.988
150	20	30	60%*FC*	0.421	0.415	0.989	0.418	0.413	0.988	0.427	0.418	0.989
150	20	30	70%*FC*	0.416	0.420	0.989	0.417	0.416	0.989	0.440	0.416	0.989
150	20	30	80%*FC*	0.432	0.415	0.989	0.425	0.418	0.989	0.439	0.418	0.989
150	15	30	80%*FC*	0.476	0.401	0.988	0.485	0.400	0.988	0.543	0.391	0.987
200	20	30	80%*FC*	0.478	0.419	0.989	0.455	0.425	0.989	0.467	0.427	0.989
100	20	30	80%*FC*	0.403	0.398	0.988	0.415	0.396	0.988	0.426	0.396	0.988
150	10	30	80%*FC*	0.599	0.367	0.986	0.584	0.372	0.986	0.599	0.372	0.986
150	10	40	80%*FC*	0.574	0.365	0.986	0.548	0.373	0.986	0.577	0.370	0.986
				Loamy sand			**Loam**			**Sandy clay loam**		
H **(cm)**	***L*** **(cm)**	***D*** **(cm)**	θ_0 **(cm³/cm³)**	a_3	b_3	R^2	a_3	b_3	R^2	a_3	b_3	R^2
150	15	20	80%*FC*	0.282	0.505	0.992	0.445	0.421	0.989	0.413	0.429	0.989
150	20	30	60%*FC*	0.232	0.521	0.992	0.406	0.418	0.989	0.384	0.424	0.989
150	20	30	70%*FC*	0.228	0.523	0.992	0.404	0.423	0.989	0.376	0.429	0.989
150	20	30	80%*FC*	0.239	0.520	0.992	0.395	0.431	0.989	0.364	0.438	0.990
150	15	30	80%*FC*	0.272	0.502	0.992	0.437	0.417	0.989	0.392	0.429	0.989
200	20	30	80%*FC*	0.244	0.535	0.993	0.420	0.437	0.990	0.401	0.442	0.990
100	20	30	80%*FC*	0.210	0.508	0.992	0.340	0.428	0.989	0.347	0.420	0.989
150	10	30	80%*FC*	0.343	0.469	0.991	0.500	0.398	0.988	0.462	0.406	0.988
150	10	40	80%*FC*	0.242	0.501	0.992	0.484	0.396	0.988	0.471	0.396	0.988
				Sandy loam								
H **(cm)**	***L*** **(cm)**	***D*** **(cm)**	θ_0 **(cm³/cm³)**	a_3	b_3	R^2						
150	15	20	80%*FC*	0.376	0.446	0.990						
150	20	30	60%*FC*	0.344	0.445	0.990						
150	20	30	70%*FC*	0.338	0.449	0.990						
150	20	30	80%*FC*	0.324	0.458	0.990						
150	15	30	80%*FC*	0.363	0.443	0.990						
200	20	30	80%*FC*	0.346	0.465	0.991						
100	20	30	80%*FC*	0.311	0.440	0.990						
150	10	30	80%*FC*	0.424	0.422	0.989						
150	10	40	80%*FC*	0.408	0.419	0.989						

by Origin 9.0; namely:

$$Z_A = 0.197(\theta_s - \theta_0)^{0.016} K_s^{-0.045} (qL)^{0.206} t^{0.476} \quad (23)$$

$$R_B = 0.694(\theta_s - \theta_0)^{-0.055} K_s^{0.008} (qL)^{0.267} t^{0.406} \quad (24)$$

$$Z_C = 0.629(\theta_s - \theta_0)^{-0.151} K_s^{0.110} (qL)^{0.229} t^{0.428} \quad (25)$$

Evaluation of the empirical model

To evaluate the accuracy of the prediction model of the soil wetting pattern size of the vertical moistube irrigation, the indoor experiments is used to verify the model, with the calculated value of the prediction model compared with the measured value (Figure 4). Based on Equations (14)–(16),

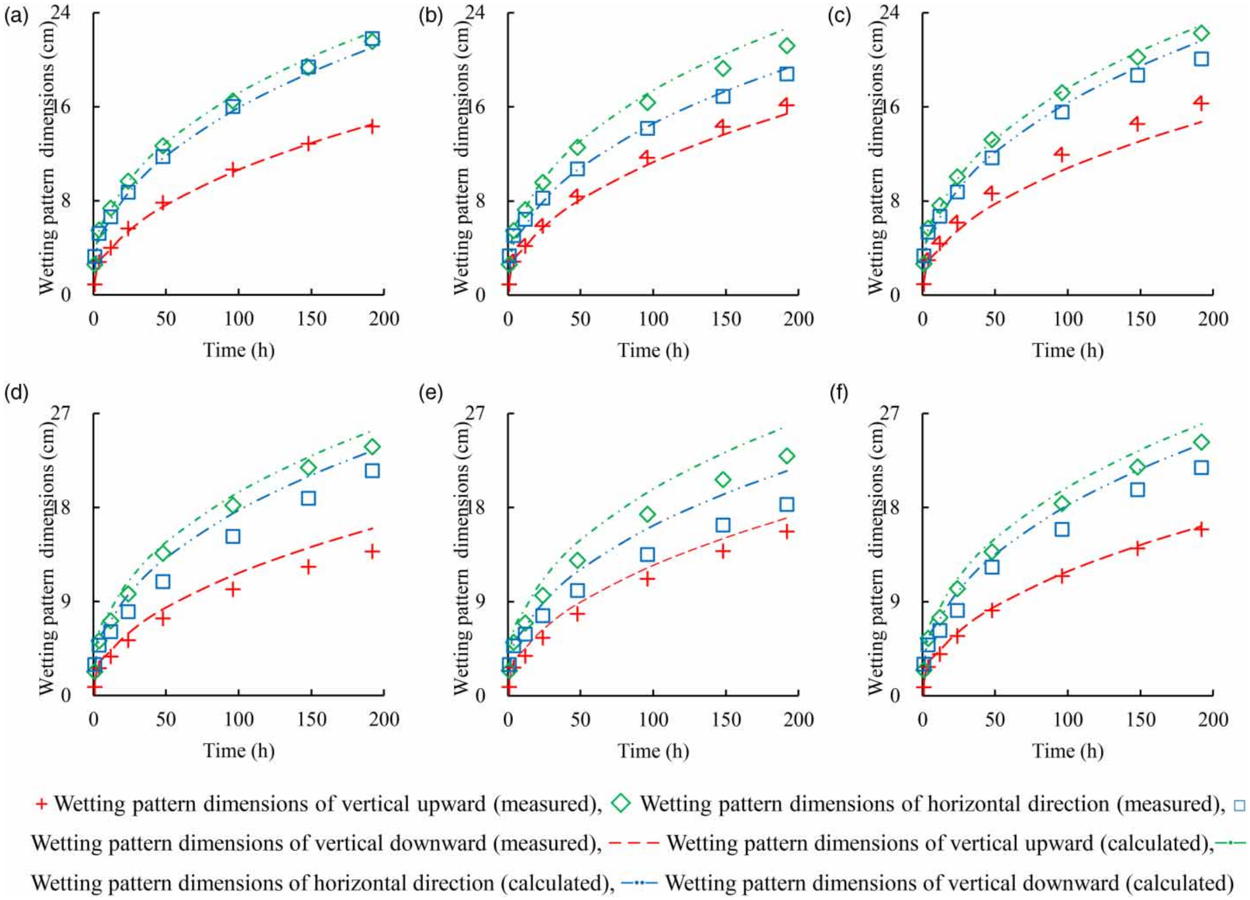

Figure 4 | Comparison between measured values and calculated values of the model. (a) Sandy loam, $L = 20$ cm, $D = 30$ cm, $H = 150$ cm; (b) silt loam, $L = 20$ cm, $D = 30$ cm, $H = 150$ cm; (c) sandy clay loam, $L = 20$ cm, $D = 30$ cm, $H = 150$ cm; (d) sandy loam, $L = 10$ cm, $D = 40$ cm, $H = 200$ cm; (e) silt loam, $L = 10$ cm, $D = 40$ cm, $H = 200$ cm; (f) sandy clay loam, $L = 10$ cm, $D = 40$ cm, $H = 200$ cm.

a statistical analysis is carried out on the calculated and measured values of the model (Table 5).

Figure 4 shows that the measured values of soil wetting pattern of vertical moistube irrigation is consistent with the calculated values of the model, but the horizontal fit is the best. It can be seen from Table 5 that MAE of the statistical indicators of the built model is between 0.30 and 1.42 cm, RMSE is between 0.42 and 1.65 cm, and NSE is not less than 0.93. This shows that the model prediction effect is good, but there are still some errors. The reason may be that when the prediction model of soil wet pattern size for vertical moistube irrigation is established, in different combinations of K_s, qL, and $(\theta_s - \theta_0)$, the power function exponent of the wetting pattern size and irrigation time varies little in

Table 5 | Statistical analysis of calculated values of the model and measured values for wetting pattern dimensions

ST	Experimental setup	MAE (cm)	RMSE (cm)	NSE
Sandy loam	$L = 20$ cm, $D = 30$ cm, $H = 150$ cm	0.30	0.42	0.99
	$L = 10$ cm, $D = 40$ cm, $H = 200$ cm	1.19	1.33	0.96
Silt loam	$L = 20$ cm, $D = 30$ cm, $H = 150$ cm	0.46	0.61	0.99
	$L = 10$ cm, $D = 40$ cm, $H = 200$ cm	1.42	1.65	0.93
Sandy clay loam	$L = 20$ cm, $D = 30$ cm, $H = 150$ cm	0.56	0.75	0.99
	$L = 10$ cm, $D = 40$ cm, $H = 200$ cm	0.94	1.19	0.97

the vertical upward, horizontal, and vertical downward direction. In order to simplify the calculation, the average values are taken, which affects the accuracy of the calculation results to a certain extent. In addition, only using the difference between K_s and (θ_s–θ_0) to characterize the size of different ST wetting patterns is also one of the reasons for the partial error. It should be noted that in the process of irrigation advancement, the wetting boundary will reach the surface and the vertical upward Equation (23) is no longer applicable, but the buried depth value can be taken when the estimated value is greater than the buried depth of the moistube. The arrival of the wetting boundary on the surface has little effect on the horizontal and vertical downward migration of wetting patterns, and Equations (24) and (25) still apply. For soils with large pores between soil particles, such as sand, the model should be used with caution.

CONCLUSIONS

On the basis of qualitative research on the influencing factors of wetting pattern of vertical moistube irrigation, this study adds the simulation quantity. The HYDRUS-2D software is used to simulate the size data of the wetting pattern under different factors. By analyzing and summarizing the laws of simulation data, a simplified empirical model for predicting the size of soil wetting patterns has been constructed, with the reliability of the model verified with experimental data. The following conclusions are obtained.

The power function is used to fit the relationship between the size of the soil wetting pattern and the irrigation time. The power function exponent varies slightly in the vertical upward, horizontal, and vertical downward directions of the moistube, with the average values taken as 0.476, 0.406, and 0.428, respectively. The power function coefficient conformed to the power function relationship with K_s, qL, and (θ_s–θ_0).

Based on this, an empirical model of the size of the vertical moistube irrigation wetting pattern was established. The model includes t, K_s, qL, and (θ_s–θ_0). The MAE of the statistical indicators of the built model is between 0.30 and 1.42 cm, RMSE is between 0.42 and 1.65 cm, and NSE is not less than 0.93. The prediction effect of the model is good, and it can provide a scientific basis for the design, operation, and management of the moistube irrigation engineering.

ACKNOWLEDGEMENTS

This study was supported by the National Natural Science Foundation of China (No. 51409137 and 51969013), the Natural Science Foundation of Gansu Province, China (No. 18JR3RA144), and Hongliu Supporting Discipline of Lanzhou University of Technology.

DATA AVAILABILITY STATEMENT

All relevant data are included in the paper or its Supplementary Information.

REFERENCES

Al-Ogaidi, A. M. A., Wayayok, A., Rowshon, M. K. & Abdullah, A. F. 2016 Wetting patterns estimation under drip irrigation systems using an enhanced empirical model. *Agricultural Water Management* **176**, 203–213.

Brandt, A., Bresler, E., Diner, N., Ben-Asher, I., Heller, J. & Goldberg, D. 1971 Infiltration from a trickle source: I. mathematical models. *Soil Science Society of America Journal* **35**, 683–689.

Carsel, R. F. & Parrish, R. S. 1988 Developing joint probability distributions of soil water retention characteristics. *Water Resources Research* **24**, 755–769.

Chu, S. T. 1994 Green-Ampt analysis of wetting patterns for surface emitters. *Journal of Irrigation and Drainage Engineering* **120**, 414–421.

Cook, F. J., Thorburn, P. J., Fitch, P. & Bristow, K. L. 2003 Wetup: a software tool to display approximate wetting patterns from drippers. *Irrigation Science* **22**, 129–134.

Dabral, P. P., Pandey, P. K., Ashish, P., Singh, K. P. & Sanjoy, S. M. 2012 Modeling of wetting pattern under trickle source in sandy soil of Nirjuli Pradesh (India). *Irrigation Science* **30**, 287–292.

Fan, Y. W., Huang, N., Zhang, J. & Zhao, T. 2018a Simulation of soil wetting pattern of vertical moistube-irrigation. *Water* **10**, 1–19.

Fan, Y. W., Shao, X. X., Wang, Y. & Gong, J. G. 2018b Empirical model for predicting wetted soil dimensions under vertical line source irrigation. *Transactions of the Chinese Society for Agricultural Machinery* **49**, 336–346.

Fan, Y. W., Zhao, T., Bai, G. L. & Liu, W. G. 2018c HYDRUS-2D simulation of soil wetting pattern with horizontal moistube-irrigation and analysis of its influencing factors. *Transactions of the Chinese Society of Agricultural Engineering* **34**, 115–124.

Fernandez-Galvez, J. & Simmonds, L. P. 2006 Monitoring and modeling the three-dimensional flow of water under drip irrigation. *Agricultural Water Management* **83**, 197–208.

Han, M., Zhao, C., Feng, G., Yan, Y. & Sheng, Y. 2015 Evaluating the effects of mulch and irrigation amount on soil water distribution and root zone water balance using HYDRUS-2D. *Water* **7**, 2622–2640.

Kanda, E. K., Senzanje, A. & Mabhaudhi, T. 2020 Soil water dynamics under moistube irrigation. *Physics and Chemistry of the Earth* **115**, 1–10.

Kandelous, M. M. & Šimůnek, J. 2010 Comparison of numerical, analytical, and empirical models to estimate wetting patterns for surface and subsurface drip irrigation. *Irrigation Science* **28**, 435–444.

Kilic, M. 2018 Analytical description of the wetting pattern in a drip irrigation system by a new method, simultaneous double parabola design. I: Method. In: *1st International Congress on Agricultural Structures and Irrigation*, Antalya, Turkey, pp. 365–375.

Malek, K. & Peters, R. T. 2011 Wetting pattern models for drip irrigation: new empirical model. *Journal of Irrigation and Drainage Engineering* **137**, 530–536.

Moncef, H. & Khemaies, Z. 2016 An analytical approach to predict the moistened bulb volume beneath a surface point source. *Agricultural Water Management* **166**, 123–129.

Moriasi, D. N., Arnold, J. G., Van Liew, M. W., Bingner, R. L., Harmel, R. D. & Veith, T. L. 2007 Model evaluation guidelines for systematic quantification of accuracy in watershed simulations. *Transactions of the ASABE* **50**, 885–900.

Naglič, B., Kechavarzi, C., Coulon, F. & Pintar, M. 2014 Numerical investigation of the influence of texture, surface drip emitter discharge rate and initial soil moisture condition on wetting pattern size. *Irrigation Science* **32**, 421–436.

Niu, W. Q., Zhang, M. Z., Xu, J., Zou, X. Y., Zhang, R. C. & Li, Y. 2017 Prediction methods and characteristics of flow for moistube. *Transactions of the Chinese Society for Agricultural Machinery* **48**, 217–224.

Pachepsky, Y. & Park, Y. 2015 Saturated hydraulic conductivity of US soils grouped according to textural class and bulk density. *Soil Science Society of America Journal* **79**, 1094–1100.

Philip, J. R. 1984 Travel times from buried and surface infiltration point sources. *Water Resources Research* **20**, 990–994.

Quinones-Bolanos, E., Zhou, H., Soundararajan, R. & Otten, L. 2005 Water and solute transport in pervaporation hydrophilic membranes to reclaim contaminated water for micro-irrigation. *Journal of Membrane Science* **252**, 19–28.

Rab, M. A., Chandra, S., Fisher, P. D., Robinson, J. N., Kitching, M., Aumann, C. D. & Imhof, M. 2011 Modelling and prediction of soil water contents at field capacity and permanent wilting point of dryland cropping soils. *Soil Research* **49**, 389–407.

Richards, L. A. 1931 Capillary conduction of liquids through porous mediums. *Journal of Applied Physics* **1**, 318–333.

Saito, H., Šimůnek, J. & Mohanty, B. P. 2006 Numerical analysis of coupled water, vapor, and heat transport in the vadose zone. *Vadose Zone Journal* **5**, 784–800.

Šimůnek, J., van Genuchten, M. Th. & Šejna, M. 2008 Development and applications of the HYDRUS and STANMOD software packages and related codes. *Vadose Zone Journal* **7**, 587–600.

Šimůnek, J., van Genuchten, M. Th. & Šejna, M. 2016 Recent developments and applications of the HYDRUS computer software packages. *Vadose Zone Journal* **15**, 1–25.

Subbaiah, R. A. 2013 Review of models for predicting soil water dynamics during trickle irrigation. *Irrigation Science* **31**, 225–258.

van Genuchten, M. Th. 1980 A closed-form equation for predicting the hydraulic conductivity of unsaturated soils. *Soil Science Society of America Journal* **44**, 892–898.

Yang, Q. 2010 *Irrigation Method with Semi Permeable Membrane, Irrigation Container and Irrigation System Made of Semi Permeable Membrane and Their Application*. EP: 2153714A1.

Yao, W. W., Ma, X. Y., Li, J. & Parkes, M. 2011 Simulation of point source wetting pattern of subsurface drip irrigation. *Irrigation Science* **29**, 331–339.

Zhang, G. X., Shen, L. X. & Guo, Y. M. 2016 Effect of soil structure on water infiltration under moistube irrigation. *Journal of Irrigation and Drainage* **35**, 35–39.

First received 7 July 2020; accepted in revised form 5 November 2020. Available online 18 November 2020